Patterning light emitting porous silicon using helium beam irradiation

E. J. Teo [a*], M. B. H. Breese [b], A. A. Bettiol [b], F. Champeaux [b] and D. J. Blackwood [a]

[a] Department of Material Science, National University of Singapore, Singapore 119260
[b] Centre for Ion Beam Analysis (CIBA), Physics Department, National University of Singapore,
Singapore 117542

ABSTRACT

High energy helium beam has been utilized to pattern silicon prior to electrochemical etching in hydrofluoric acid. Photoluminescence (PL) studies carried out on medium resistivity silicon showed that the PL wavelength of the irradiated regions is continuously red-shifted by up to 150 nm with increasing dose. On the lower resistivity silicon, the intensity is shown to increase by more than twenty times with dose. Atomic force microscopy (AFM) and scanning electron microscopy (SEM) have been used to determine the surface morphology of the irradiated structure. This technique is potentially important for producing an integrated silicon based optoelectronic device.

Keywords: light emitting porous silicon, ion beam irradiation, photoluminescence.

1. INTRODUCTION

Due to its indirect bandgap, silicon is not a suitable material for fabrication of photonic devices. This limits the integration of silicon photonic devices into standard microelectronics. With the discovery of strong visible light emission from porous silicon[1], new possibilities of using silicon for photonic applications are intensively studied[2].

Porous silicon is typically produced by electrochemical anodization of silicon wafer in a hydrofluoric acid electrolyte[3]. The hole current flowing to the surface facilitates the partial dissolution of silicon. This results in the formation of highly porous silicon skeleton, which exhibits strong photoluminescence band centred around 1.4-1.9 eV (600-800nm). It is able to emit at energies higher than the bandgap of silicon, probably due to the quantum confinement effects produced by the low dimensionality of the silicon skeleton remaining after anodization.

Various methods have been employed to alter the peak wavelength of light emitting porous silicon, e.g. by changing the etching current densities[3], oxidation[4] or photochemical etching[5,6]. To alter the light emitting properties of porous silicon on a micron scale, patterning techniques such as optical[7], photolithographic[8], electron[9], soft lithography[10] or ion beam irradiation[11-14] have been used. The use of light or electrons often result in selective enhancement or quenching of PL intensity but not so much the PL wavelength. In contrast, ion irradiation is able to alter the resistivity of silicon, which affects the wavelength as well as the intensity [11,14].

In this work, we employ 2 MeV helium ions to pre-irradiate the silicon instead of lower energy, heavier ions used in previous studies. According to SRIM calculations [15], the damage created is 2-3 orders of magnitude lower than that of 300 keV Si ions, and extends to a depth of 7 μm rather than 400 nm. This provides greater control over the resultant PL emission due to the thicker damaged layer and reduced rate of damage with dose. We aim to produce patterned micron-sized areas of porous silicon with varying PL wavelength and intensities on a single substrate.

---

* Corresponding author: Teo Ee Jin Email: msetej@nus.edu.sg; Tel: +65 65164299, Fax: +65 67776126

2. EXPERIMENTAL

Three different resistivity p-type silicon wafers were patterned with a focused beam of 2 MeV helium ions in a nuclear microprobe16,17. After irradiation, a contact was made to the back surface using Ga-In eutectic and copper wire. The wafers were anodized at a current density of 100 mA/cm2 for 5 minutes in a HF:ethanol:water electrolyte in the ratio 1:2:1, producing a porous layer several microns in thickness. The wafers were then washed in distilled water followed by ethanol and transferred immediately to a vacuum chamber. By dwelling a longer time at each particular region, the damage created by the beam can be increased so that the rate of porous silicon formation is reduced. This results in a thinner layer of porous silicon formed (see figure 1b) at higher dose irradiation.
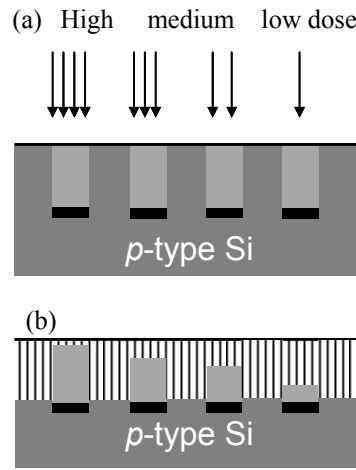

Figure1. Schematic diagram showing the experimental procedure. (a) 2 MeV helium beam irradiation into p-type Si followed by (b) porous silicon formation in hydrofluoric acid.

Micro-PL spectroscopy was carried out on the patterned porous silicon using a 405 nm diode laser with an output power of 1-2 mW. The laser light was focused through a ME600 Nikon microscope onto the sample. The PL signals were then detected using a CCD Ocean Optics Spectrometer by means of an optical fiber. Most of the laser light was cut off from the PL signal with 495 nm long-pass filter. All spectra have been corrected for system response. For PL imaging, the samples are excited with a UV lamp through a 400 nm filter and captured with a charge-coupled device(CCD) camera. All measurements have been carried out in a vacuum chamber.

3. RESULTS

### 3.1. Effect of ion irradiation on the resistivity of silicon

Ion irradiation introduces lattice damage to the silicon in the form of vacancy-interstitial pairs. For 2 MeV helium ions, the density of defects is fairly constant for the first 6 μm of the trajectories and then increases sharply towards the end of range at 7 μm [15]. These defects may form trap levels in the energy bandgap where charge carriers can undergo recombination. This reduces the hole density and increases the resistivity. Based on the measured values of defect production and trapping rates published in ref 18, the resistivity as a function of 2 MeV He ion dose has been plotted in figure 2, taking into account the changes in hole mobility with doping concentration. Both curves show a sudden increase in resistivity above a certain dose threshold. The change in resistivity for the low resistivity silicon occurs at a much higher dose of 10^{14}-10^{15}/cm^2 as compared to 10^{12}-10^{13} /cm^2 for medium resistivity silicon.
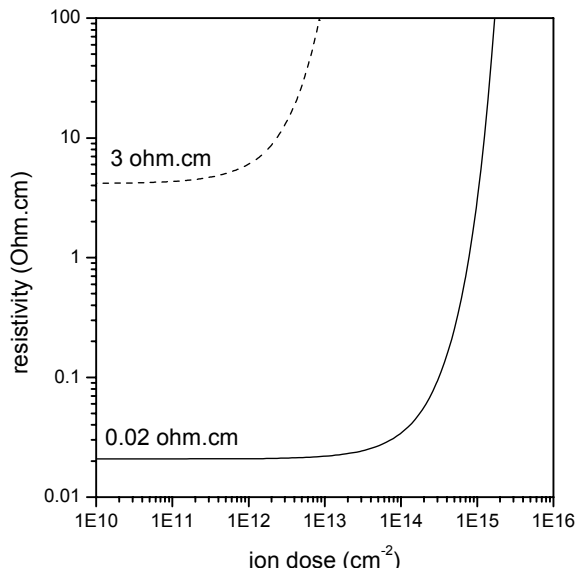
Figure 2. Calculated resistivity close to the surface of *p*-type silicon as a function of 2 MeV helium ion dose, for 0.02 Ω.cm and 3 Ω.cm *p*-type silicon wafers.

3.2. Effect of ion beam irradiation on silicon with resistivity of 0.02Ω.cm

A highly focused 2 MeV helium beam has been used to irradiate heavily doped p-type silicon of 0.02Ω.cm resistivity. The sample was then etched at 50 mA/cm^2 for 5 min. Figure 3 shows the PL image of a series of squares irradiated with doses from 2×10^{13} to 5×10^{15}/cm^2. The dotted squares in the lower dose irradiations are drawn to guide the eye and the increase of dose is indicated by the direction of the arrow shown in the image. It is clearly seen that the ion irradiation enhances the PL emission of the porous silicon. Initially, the intensity increases for doses up to 2×10^{15}/cm^2 and then it starts to drop with further increase in dose.
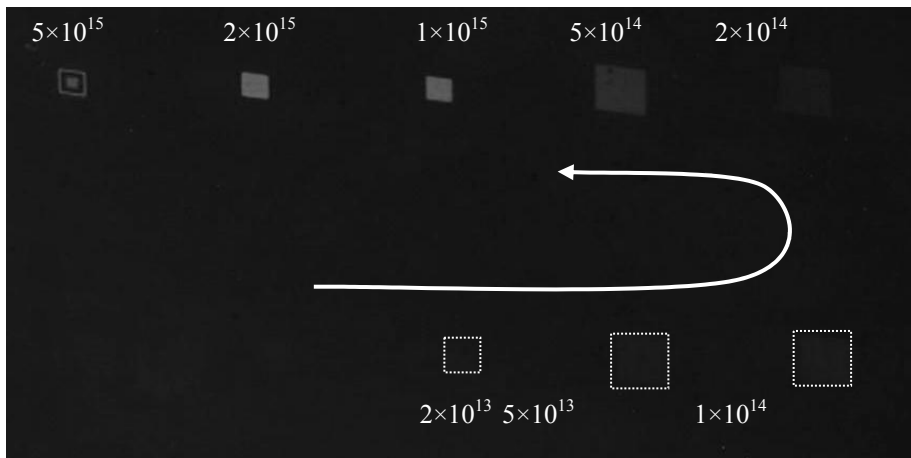

Figure 3. PL image of the irradiated squares formed on 0.02 Ω.cm resistivity.
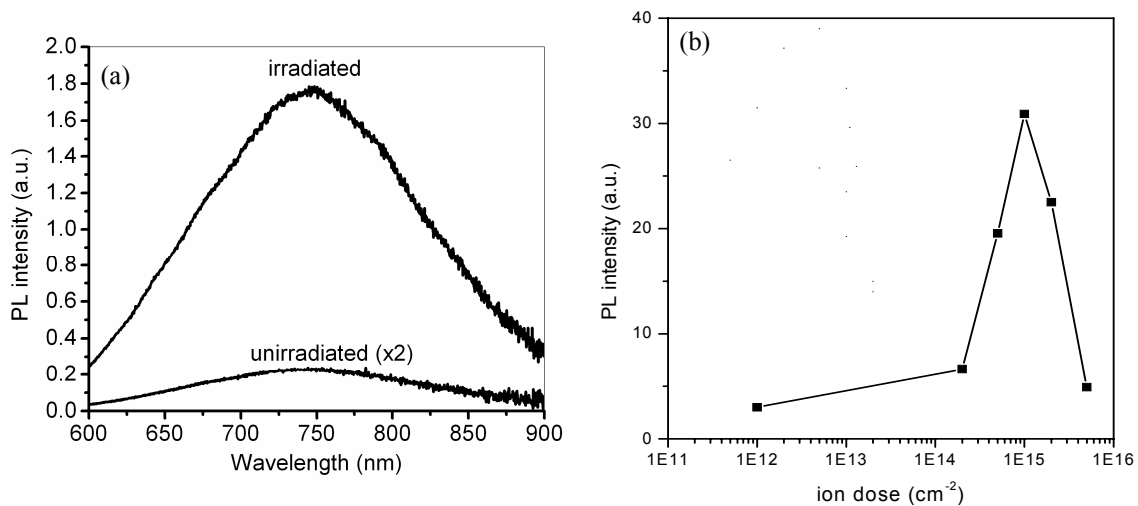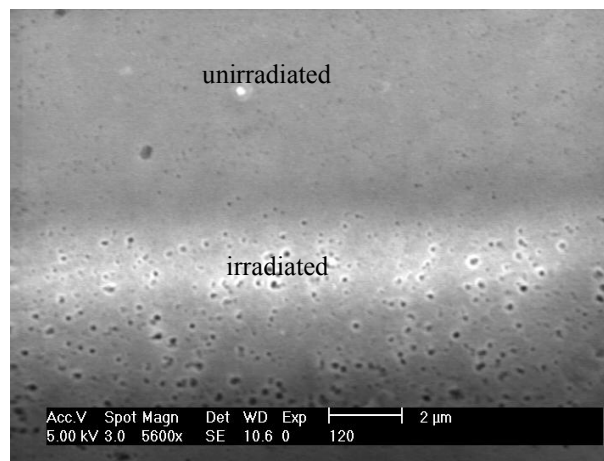
Figure 4. (a) PL spectra of the irradiated and unirradiated regions. (b) Plot of PL intensity vs dose.

Micro-PL measurements of the irradiated regions shows that the emission has a broad FWHM of 200 nm with a peak wavelength of 750 nm. This suggests the presence of a wide distribution of pore sizes. Very low PL signal is observed from the unirradiated regions, with no significant shift in wavelength as compared to the irradiated regions. It is also shown that the resistivity change is significant enough to produce a peak intensity of 20× higher than the unirradiated regions. In earlier studies carried out by Gaburro *et.al.*[19], it is shown that the PL intensity depends strongly on the resistivity of *p*-type silicon. Much higher PL emission was observed on samples with resistivity of 1-10 Ω.cm compared to 0.01 Ω.cm. The PL intensity is extracted from each irradiated square to determine its dependency on dose (see figure 4b). Significant increase in the PL intensity is observed for doses from 2×10^{14} to 1×10^{15} /cm^2. After which, the intensity starts to reduce again. This dose regime corresponds well with the sudden increase of the silicon resistivity seen in figure 2.

AFM measurements are carried out to investigate the morphology of the irradiated and unirradiated regions. It is found that the irradiated region has a root-mean-square roughness (RMS) of 9.4 nm, whereas the RMS roughness of the unirradiated region is 5.7 nm. Line profile across the structure shows that the unirradiated region is raised 47 nm above the irradiated region. This implies that the porous silicon formed in the irradiated region has a higher porosity, resulting in loss of volume and height. Scanning electron microscopy (SEM) of the structure in figure 6 also reveals that the surface contains more voids in the irradiated regions as compared to the unirradiated regions.
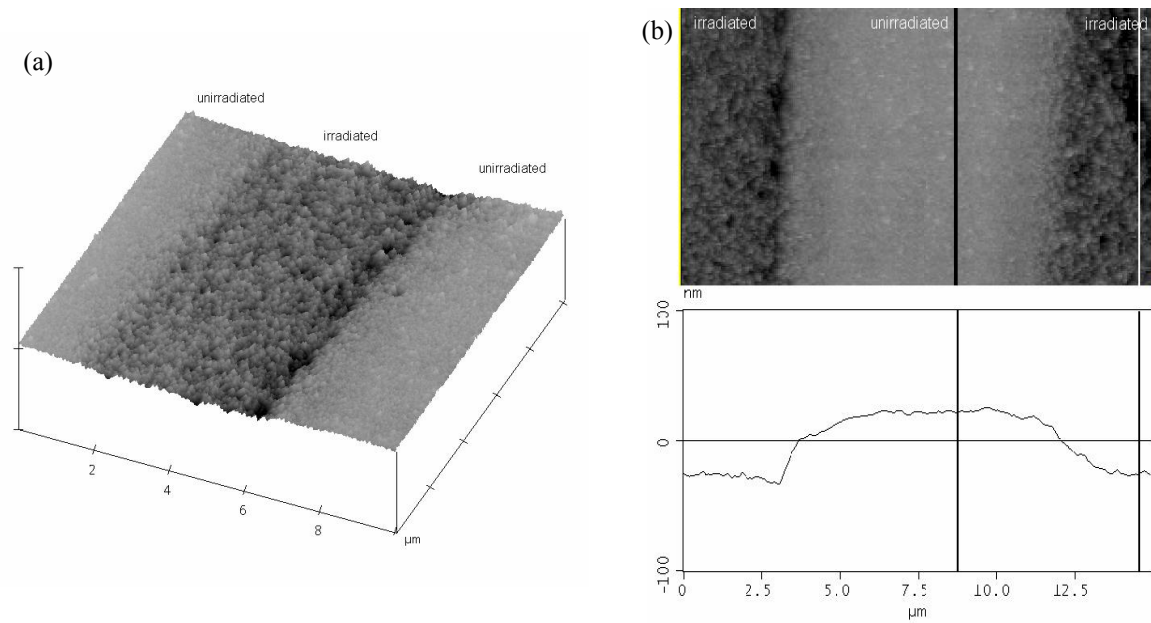
Figure 5. (a) A 10×10 μm AFM image of an irradiated structure. (b) Line profile across the irradiated structure.

Figure 6: Close up SEM of the irradiated and unirradiated regions of porous silicon.

We have demonstrated the versatility of this direct writing process by fabricating some complex patterns shown in figure 7. Figure 7a is a grid pattern, consisting of five horizontal bars overlapped with five vertical bars. The dwell time of the beam at each region can be accurately controlled to irradiate each bars at 2, 4, 6, 8, $10 \times 10^{15}/cm^2$, increasing in the direction of the arrows shown in figure 7a. The overlapped regions appear brighter in the form of squares. In figure 7b, we have irradiated a complex image of a dragon with a resolution of 1 μm.
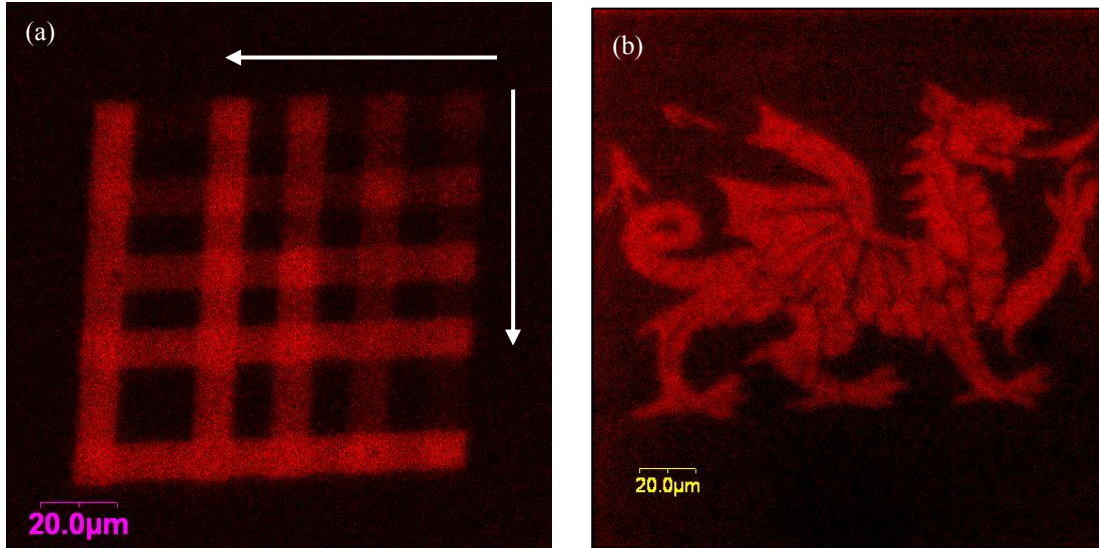
Figure 7. (a) A grid pattern irradiated with different doses (b) A PL image of a dragon irradiated with a dose of 1×10^{15} /cm^2.

3.3. Effect of ion beam irradiation on medium resistivity silicon

Ion irradiation studies on silicon with resistivity of 0.3 and 3 Ω.cm have been carried out using a 2 MeV He beam. Both samples have been irradiated with a series of six squares with a dose of 5×10^{11}, 1×10^{12}, 2×10^{12}, 5×10^{12}, 1×10^{13}, 2×10^{13} /cm^2. The sizes of the squares with higher irradiation doses are reduced so that the dose can be increased with the same current setting. There is a noticeable red-shift in wavelength emission of the porous silicon with irradiation (see figure 8). As the dose increases, the yellowish background from the 0.3Ω.cm porous silicon is shifted towards the red colour. On the 3 Ω.cm silicon, the green background is shifted towards yellow, orange and then red as the dose increases from 5×10^{11} to 1×10^{13} /cm^2. According to previous measurements[3,19], the PL wavelength is at a minimum for wafers with moderate resistivity of 0.1-10Ω.cm, where anodization produces a large fraction of microporous silicon with silicon islands of < 2nm. Quantum confinement effects are expected to dominate when electrons are confined to volume less than the exciton radius of 4.9 nm for silicon. Anodization of lower resistivity silicon produces a significant fraction of mesopores and micropores which are bigger in size. This explains the much weaker PL intensity observed from the background in figure 3.
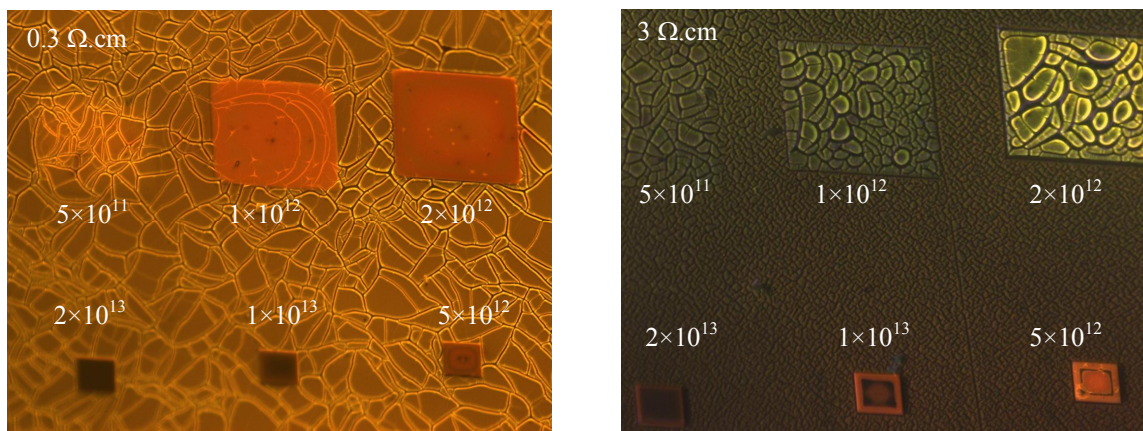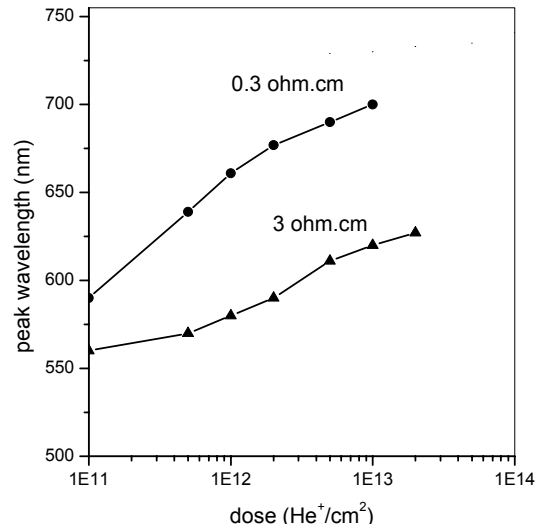

Figure 8. PL images of 0.3 and 3 Ω.cm resistivity silicon irradiated with squares of different doses.

In order to determine the change in PL wavelength with dose, micro-PL measurements are carried out on each square and plotted in figure 9. It is shown clearly that the wavelength of the emission can be tuned within a dose range of 1×10^{11} to 1×10^{13} /cm^2. The PL wavelength is continuously red-shifted by up to 150 nm for the 0.3 Ω.cm silicon. For doses higher than 2×10^{13} /cm^2, the PL intensity becomes much lower and cannot be detected by the spectrometer. It should be noted that the cracking observed in these films can be reduced by carrying out proper by freeze or supercritical drying.

Figure 9. Plot of peak wavelength vs dose for porous silicon formed on 0.3 and 3 Ω.cm resistivity silicon.

We have irradiated concentric ring patterns whereby the dose of each ring is gradually varied in a radial manner. Figure 10 show the PL images of the resultant circular patterns formed on 3 Ω.cm and 0.3 Ω.cm Si. On the 3 Ω.cm Si, the green colour is slowly red-shifted towards red as the dose increases from 10^{12} /cm^2 at the side to 1.3×10^{13} /cm^2 at the centre, producing a multi-colour pattern. A similar pattern has been fabricated on 0.3 Ω.cm Si, but with the dose increasing towards the side and this time the colour of emission is seen shifting from red to deep red.
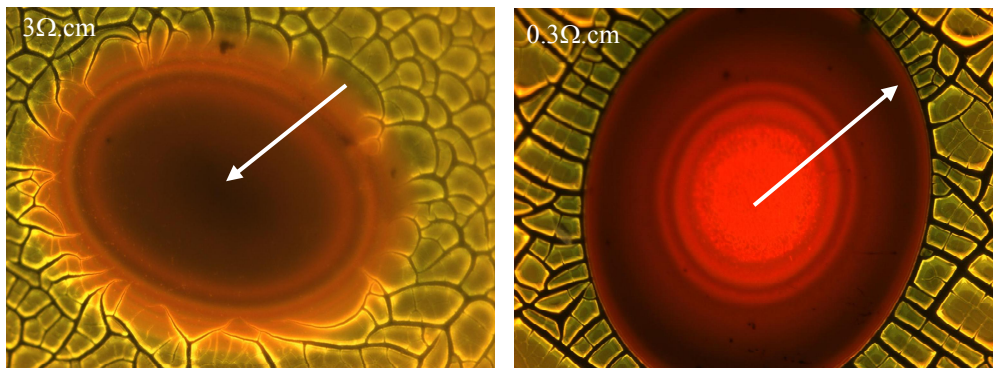
Figure 10. PL image of concentric ring pattern with doses increasing in the direction of the arrows.

4. CONCLUSIONS

Focused 2 MeV helium irradiation has been used to pattern porous silicon for tunable PL wavelength and intensity emission. Significant increase in the PL intensity has been observed on the low resistivity silicon as the dose increases to 10^{15} /cm^2. AFM and SEM results indicate that the increase in PL intensity is probably due to the higher porosity of porous silicon formed in the irradiated regions, as a result of increased resistivity. For the medium resistivity silicon, the PL results show a significant red-shift in wavelength. Currently, Raman spectroscopy is being carried out to determine the origin of the red-shift in wavelength with irradiation. The technique enables us to create patterned porous silicon with widely varying wavelength and intensities by accurate control of the beam dose.

REFERENCES

1. L. T. Canham, Appl. Phys. Lett. **57,** 1046 (1990)
2. K. D. Hirschman, L. Tsybeskov, S. P. Duttagupta, P. M. Fauchet, *Nature* **1996,** *384*, 338.
3. *Electrochemistry of Silicon* (Ed: V. Lehmann), Wiley-VCH, Weinheim **2002**.
4. A. J. Kontkiewicz, A. M. Kontkiewicz, J. Siejka, S. Sen, G. Nowak, A. M. Hoff, P. Sakthivel, K. Ahmed, P. Mukherjee, S. Witanachchi and J. Lagowski, *Appl. Phys. Lett.* 65, 1436, 1994.
5. H. Mizuno, H. Koyama and N. Koshida, *Appl. Phys. Lett*. 69, 3779, 1996.
6. M. V. Wolkin, J. Jorne, P. M. Fauchet, G. Allan and C. Delerue*, Phys. Rev. Lett*, 82, 197, 1999.
7. V. V. Doan, M. J. Sailor, *Science* **1992,** *256*, 1791.
8. S. P. Duttagupta, C. Peng, P. M. Fauchet, S. K. Kurinec, T.N. Blanton, *J. Vac. Sci. Technol. B* **1995,** *13*, 1230.
9. M. Rocchia, S. Borini, A. M. Rossi, L. Boarino, G. Amato, *Adv. Mater.* **2003**, *15*, 1465.
10. D. J.Sirbuly, G. M. Lowman, B. Scott, G. D. Stucky, S. K. Buratto, *Adv. Mater.* **2003**, *15*, 149
11. X. M. Bao, H. Q. Yang, F. Yan*, J. Appl. Phys.* **1993,** *79*, 1320.
12. S. Chattopadhyay, P. W. Bohn, *J. Appl. Phys.* **2004,** *96***,** 6888.
13. E. J. Teo, D. Mangaiyarkarasi, M. B. H. Breese, A. A. Bettiol, D. J. Blackwood, *Appl. Phys. Lett.* **2004,** *85*, 4370.
14. L. Pavesi, G. Giebel, F. Ziglio, G. Mariotto, F. Priolo, S. U. Campisano, C. Spinella, *Appl. Phys. Lett.* **1994,** *65*, 2182.
15. *The Stopping and Range of Ions in Solids.* (Ed: J. F. Ziegler, J. P. Biersack, U. Littmark), Pergamon Press, New York **1985**.
16. *Materials Analysis using a Nuclear Microprobe* (Ed: M. B. H. Breese, D. N. Jamieson, P. J. C. King), Wiley, New York **1996**.
17. J.A. van Kan, A. A. Bettiol, F. Watt, A*ppl. Phys. Lett.* **2003,** *83*, 1629.
18. M. Yamaguchi, S. J. Taylor, Yang, S. Matsuda, O. Kawasaki, T. Hisamatsu, *J. Appl. Phys.* **1996,** *80***,** 4916.
19. Z. Gaburro, H. You, D. Babic, J. Appl. Phys. **84,** 6345 (1998).